

# Summarized General Scaling Laws Covering Over the Representative Tandem-Mirror Operations in GAMMA 10

T. Cho, M. Hirata, H. Hojo, M. Ichimura, K. Ishii, A. Itakura, I. Katanuma, J. Kohagura, Y. Nakashima, T. Saito, S. Tanaka, Y. Tatematsu, M. Yoshikawa, T. Tamano, K. Yatsu, and S. Miyoshi

Plasma Research Centre, University of Tsukuba, Tsukuba, Ibaraki 305-8577, Japan

e-mail: tcho@prc.tsukuba.ac.jp

**Abstract.** *Generalized scaling laws* covering over the representative tandem-mirror operational modes from 1979 to 2000 in GAMMA 10 [*i.e.*, characterized in terms of (i) a *high-potential mode* having kV-order ion-confining potentials ( $\phi_c$ ) and thermal-barrier potentials ( $\phi_b$ ), and (ii) a *hot-ion mode* yielding fusion neutrons with 10-20-keV bulk-ion temperatures] are found and summarized for providing the possibilities of combining the characteristics from each mode into novel extended operational modes. The physics scalings of the formation of the plasma confining potentials as well as the associated effects of the potentials on plasma-parameter improvements are systematically investigated as follows: (i) The *potential-formation scalings* in the two representative modes are consolidated and generalized on the basis of the consistency with the novel findings of wider validity of *Cohen's strong electron-cyclotron heating (ECH) theory* covering over both modes. (ii) The *produced potentials*, in turn, provide a favorable *novel scaling of the increase in the central-cell electron temperatures  $T_e$  with increasing  $\phi_b$* , limited by the available ECH powers. The scaling of  $T_e$  with  $\phi_b$  is well interpreted by the *Pastukhov theory* of plasma potential confinement, as a similarly reported scaling of potential-confined ion temperatures with  $\phi_c$ . (iii) A scaling of  $\phi_c$  [kV] with ECH powers in a plug region,  $P_{ECH}$  [kW], and the central-cell densities,  $n_c$  [ $10^{18} \text{ m}^{-3}$ ], is summarized as  $\phi_c = 1.73 \times 10^{-4} P_{ECH}^{1.73} \exp(-0.33n_c)$ . (iv) Consequently, under the assumption of the validity of the extension of these theoretically well interpreted scaling data, the formation of Pastukhov's predicted  $\phi_c$  of 30 kV for confining  $Q=1$  plasmas is scaled to require 5-MW  $P_{ECH}$ .

## 1. Introduction

Generalized and extended scaling laws covering over the representative tandem-mirror operational modes are summarized for clarifying the present status in GAMMA 10 and for providing innovative approaches to alternative fusion-energy achievement. The main tandem-mirror operations from 1979 to 2000 in GAMMA 10 are characterized in terms of (i) a high-potential mode having kV-order plasma-confining potentials [1,2], and (ii) a hot-ion mode yielding fusion neutrons with 10-20 keV bulk-ion temperatures [3,4]. In this manuscript, a large number of database obtained from these two main GAMMA10 operations is intensively investigated and summarized to highlight the common essential physics bases underlying in both modes. In particular, systematic researches into the formation of plasma-confining potentials and the associated effects of the potential formation on the improvements in plasma parameters are carried out.

## 2. Experimental Apparatus

GAMMA 10 is a minimum- $B$  anchored tandem mirror with outboard axisymmetric plug and barrier cells [1-4]. It has an axial length of 27 m, and the total volume of the vacuum vessel is  $150 \text{ m}^3$ . The central cell has a length of 6 m and a fixed limiter with a diameter of 0.36 m, and the magnetic-field intensity at the midplane  $B_m$  is 0.405 T with a mirror ratio  $R_m$  of 5.2. Ion-cyclotron heatings (ICH) (200 kW at 4.47 or 6.36 MHz, as well as 100 kW at 9.9 or 10.3 MHz) are employed for the central-cell hot-ion production and the anchor stabilization, respectively. The plug and barrier cells are axisymmetric mirrors; they have an axial length of 2.5 m ( $B_m=0.497$  T, and  $R_m=6.2$ ). Microwaves (150 kW at 28 GHz) are injected in the

extraordinary mode into the plug and the barrier regions to produce an ion-confining potential  $\phi_c$ , and a thermal-barrier potential  $\phi_b$ , respectively. Plug potentials  $\Phi_p$  are measured with originally developed electrostatic spectrometer arrays for end-loss-ion energy analyses (ELA). Central-cell potentials  $\Phi_c$  and barrier potentials  $\Phi_B$  are directly measured with heavy-ion ( $\text{Au}^0$ ) beam probes (HIBP). Therefore, one can obtain  $\phi_c$  and  $\phi_b$ , as  $\Phi_p - \Phi_c$  and  $\Phi_c - \Phi_B$ , respectively. X-ray diagnostics give profiles of electron temperatures  $T_e$  along with detailed electron-energy spectra in each region [2].

### 3. Scaling Law of the Formation of Thermal-Barrier and Ion-Confining Potentials

Figure 1 stands for one of *the most essential scalings of potential formation*. The scaling law of ion-confining potentials  $\phi_c$  with thermal-barrier potentials  $\phi_b$  in the high-potential mode [Fig. 1(a)] is compared to the scaling in the hot-ion mode [Fig. 1(b)]. Both scalings show favorable similar characteristics of remarkably growing  $\phi_c$  with increasing thermal transport-barrier depth  $\phi_b$ .

Careful notice, however, finds out the different dependence on the ratio of the plug to central-cell densities,  $n_p/n_c$ , despite the similarly behaved relations between  $\phi_c$  and  $\phi_b$ . This is contrary to the standard prediction from Cohen's theory of potential formation [5]. (Plotted data have the parameter regime of  $n_p/n_c$  labeled with the curves.) Existence of different underlying physics for these two typical operations could result in no chances of the upgraded innovations of combined modes.

However, *a new finding* of the synthesized generalization of these two scalings of  $\phi_c$ ,  $\phi_b$ , and  $n_p/n_c$  is achieved due to the inclusion of the scaling of central-cell electron temperatures  $T_e$  [keV] with  $\phi_b$  [kV]. The empirical scalings of  $T_e = 0.23\phi_b + 0.03$  and  $T_e = 0.16\phi_b + 0.01$  in the high-potential and hot-ion modes, respectively, (see Fig. 2) are introduced to reduce  $T_e$  in Cohen's strong ECH theoretical formula of  $\phi_c = T_e [0.665(n_p/n_c) \exp(1.19\phi_b/T_e)]^{2/3} - \phi_b$  [2,5] for plotting the solid curves labeled  $n_p/n_c$  in Figs 1(a), and 1(b), respectively. The curves well trace the data in Figs 1(a), and 1(b). In Fig. 1(c), the data sets of  $\phi_c$ ,  $\phi_b$ , and  $n_p/n_c$  in Figs 1(a) and 1(b) are replotted using the same symbols. It is found that the data lie well on each curved surface labeled (a) and (b) calculated from the strong ECH theory along with the empirical scalings of  $T_e$  with  $\phi_b$ , respectively. These methods and plots in *the proposed novel three-dimensional space* ( $\phi_c$ ,  $\phi_b$ , and  $n_p/n_c$ ), thus, address the misunderstanding of no dependence of the relation between  $\phi_c$  and  $\phi_b$  on  $n_p/n_c$ . Therefore, *the new finding of the existence of common physics relation among  $\phi_c$ ,  $\phi_b$ , and  $n_p/n_c$  in*

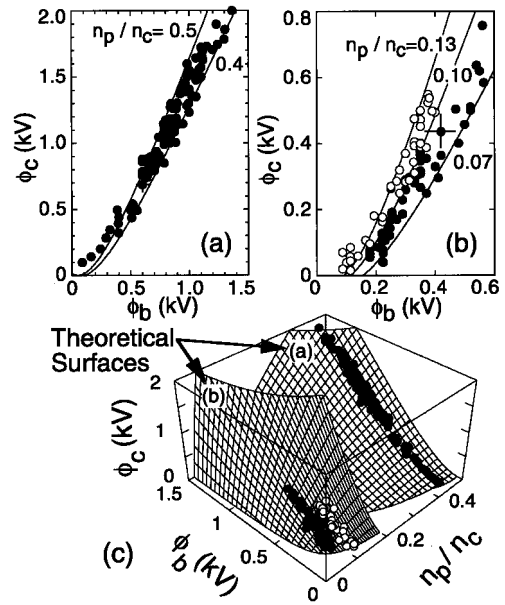


FIG. 1. The Scaling laws of ion-confining potentials  $\phi_c$  with thermal-barrier potentials  $\phi_b$  in (a) the high-potential and (b) the hot-ion modes. The data having the ratio of the plug to the central-cell densities  $n_p/n_c$  in 0.4-0.5 for (a), as well as in 0.07-0.10 (filled circles) and 0.10-0.13 (open circles) for (b) are plotted. In (c), the generalized scaling surfaces (a) and (b) in the proposed three-dimensional space of  $\phi_c$ ,  $\phi_b$ , and  $n_p/n_c$  are calculated from Cohen's strong ECH theory in combination with the scaling of  $T_e$  [keV] with  $\phi_b$  [kV] [i.e., (a)  $T_e = 0.23\phi_b + 0.03$ , and (b)  $T_e = 0.16\phi_b + 0.01$  (see FIG. 2)]. The data in (a) and (b) are well replotted using the same symbols on the theoretical surfaces of (a) and (b) in (c), respectively.

both modes encourages us to realize the possibilities of combining the characteristics in each mode for opening an innovative mode having high-potential and hot-ion properties simultaneously. Furthermore, the validity of this extended scaling theory is supported by a new finding of the theoretically predicted plateau-electron formation [5] measured with plug X-ray energy spectra for both modes.

#### 4. Scaling Law of Central-Cell Electron Temperatures with Thermal-Barrier Potentials

The scalings of  $T_e$  increasing with increasing the thermal-transport barrier depth  $\phi_b$  are shown in Figs 2(a) and 2(b) for the high-potential and hot-ion modes, respectively. In Fig. 2(a), data on axis with the warm-electron temperatures  $T_{ew}=1-2$  keV and the density ratio  $n_{ew}/n_c=0.01-0.05$  to  $n_c=(4-6)\times 10^{17} \text{ m}^{-3}$  are plotted. Ion temperatures  $T_i=2$  keV, and the neutral-particle populations  $n_0=(1-4)\times 10^{15} \text{ m}^{-3}$  are observed. Here,  $n_0$  decreases with increasing  $T_e$ . In Fig. 2(b), data having  $T_i=1-5$  keV,  $n_c=(1-2)\times 10^{18} \text{ m}^{-3}$ ,  $n_0=(1-4)\times 10^{15} \text{ m}^{-3}$ , and  $T_{ew}=1$  keV with  $n_{ew}/n_c=0.005-0.01$  are plotted. At this time,  $T_e$  increase up to 250 eV with increasing  $\phi_b$  is limited by ECH powers for potential formation (150 kW in Fig. 2) and by no direct auxiliary central-cell electron heatings.

In order to find out the common physics interpretations covering over the scaling data in Figs 2(a) and 2(b), theoretical analyses are carried out by the use of the power- and particle-balance equations (1) and (2), respectively.

$$\frac{dWV_{BB}}{dt} = P_{wb}V_{BB} + P_{hb}V_h - \frac{WV_{BB}}{\tau_E}, \quad (1)$$

and

$$\frac{dn_c}{dt} = n_0 n_c \langle \sigma v \rangle - \frac{n_c}{\tau_p}, \quad (2)$$

where  $W$  and  $\langle \sigma v \rangle$  denote the bulk-electron energy density of  $3/2n_c T_e$ , and the ionization cross section, respectively. Slowing-down power densities to the bulk electrons from the warm electrons, and the hot ions are defined as  $P_{wb}$  and  $P_{hb}$ , respectively. The volume of the warm electrons, flowing from the plug region and thus existing between both barrier regions, is denoted by  $V_{BB}$ . Diamagnetic-loop-array signals for hot-ion profile measurements are analyzed to identify the axial profile and the volume of hot ions  $V_h$ .

In Fig. 2(a), the solid curves labeled  $n_{ew}/n_c=1$  and 4% having  $T_{ew}=1$  keV are calculated from Eq. (1) with the substitution of Pastukhov's energy-confinement time [6] into  $\tau_E$ . Here, the second term of the right-hand side of Eq. (1) is one-order-of-magnitude smaller than the first term (2 keV ions with  $V_h/V_{BB}$  of 0.39). The dashed curves are simulated from Eq. (2) with

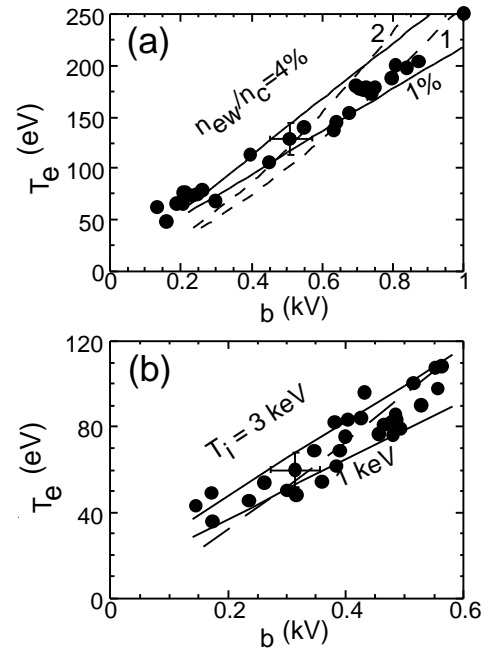


FIG. 2. The scalings of  $T_e$  with  $\phi_b$  in (a) the high-potential and (b) the hot-ion modes are fitted by the solid and dashed curves from Eqs. (1) and (2), respectively, using Pastukhov's energy and particle confinement times along with the labeled values of the ratio of the warm to bulk-electron densities  $n_{ew}/n_c$ ,  $T_i$ , or neutral-particle populations  $n_0$  [1 and 2 in (a) corresponding to 1 and  $2\times 10^{15} \text{ m}^{-3}$ , respectively, and in (b) being  $2\times 10^{15} \text{ m}^{-3}$ ] (see text). In (a), data with  $T_{ew}=1-2$  keV,  $n_{ew}/n_c=1-5\%$  [ $n_c=(4-6)\times 10^{17} \text{ m}^{-3}$ ],  $T_i=2$  keV, and  $n_0=(1-4)\times 10^{15} \text{ m}^{-3}$ ; and in (b), data with  $T_i=1-5$  keV,  $n_c=(1-2)\times 10^{18} \text{ m}^{-3}$ , and  $n_0=(1-4)\times 10^{15} \text{ m}^{-3}$  are plotted.

Pastukhov's particle-confinement time [6] into  $\tau_p$ . The tendency of increasing neutral-shielding effect with increasing  $T_e$  or  $\phi_b$  is seen by the data from  $\phi_b$  0.8, through 0.5, and then to 0.2 kV, since these data are traced by the dashed curves labeled 1 and 2 [corresponding to  $n_0=1$ , and  $2 \times 10^{15} \text{ m}^{-3}$ , respectively], and then the calculations with poorer shielding with  $n_0$   $5 \times 10^{15} \text{ m}^{-3}$ , respectively. This behavior is consistently understood by the dependence of  $\sigma_v$  on  $T_e$ . Similarly, data in Fig. 2(b) are also fitted by the calculated solid curves from Eq. (1) with  $T_i=1$  and 3 keV along with  $n_c=1.5 \times 10^{18} \text{ m}^{-3}$ . In contrast to the parameter regime in Fig. 2(a),  $P_{hb}V_h$  dominates over  $P_{wb}V_{BB}$ . In Fig. 2(b), the dashed curve is similarly estimated from Eq. (2) by the use of the averaged data of  $n_0=2 \times 10^{15} \text{ m}^{-3}$  and the above-described parameters.

Good agreement between the data and the calculated results in each different parameter regime with the different dominant-heating source in Figs 2(a) and 2(b) provides a *novel finding of the validity of the Pastukhov theory on electron energy and particle confinement*. The scaling validation *confirms the importance and effectiveness of the formation of  $\phi_b$  to confine and heat up tandem-mirror central electrons*. On the other hand, the similar effects of  $\phi_c$  on ions have already been reported [1].

In this context, we investigate to find the general formula for the relation between  $T_e$  and  $\phi_b$  on the basis of the combination of the energy-balance equation with Pastukhov's energy confinement time [6] in place of the two empirical scalings of  $T_e$  with  $\phi_b$  employed in Fig. 1. In a quasi-steady state, one can obtain the following equation when equalizing  $\tau_E$  from the Pastukhov theory [6] with  $\tau_E$  in the energy-balance equation (1) under the assumption of the predominant loss in the axial direction compared to losses including the radial direction.

$$f(x) = \frac{2.01 \cdot 10^4 n_c^2 \ln \Lambda}{T_e^{1/2} \left[ \frac{V_h}{V_{BB}} P_{hb} + P_{wb} \right]}, \text{ or } x = \frac{\phi_b}{T_e} = f^{-1} \left[ \frac{2.01 \cdot 10^4 n_c^2 \ln \Lambda}{T_e^{1/2} \left[ \frac{V_h}{V_{BB}} P_{hb} + P_{wb} \right]} \right], \quad (3)$$

where the units of  $T_e$ ,  $\phi_b$ ,  $n_c$ ,  $P_{hb}$  and  $P_{wb}$  are in keV, kV,  $10^{18} \text{ m}^{-3}$ ,  $\text{W} \cdot \text{m}^{-3}$ , and  $\text{W} \cdot \text{m}^{-3}$ , respectively, and  $x$  is defined as  $\phi_b/T_e$ .

From Eq. (3), one can reproduce the above-mentioned two empirical scalings of  $T_e$  with  $\phi_b$ . A finding of a good approximation of  $f^{-1}(x) = 0.04 + 0.97 \ln [f(x)]$  along with the substitution of standard formula for  $P_{hb}$  and  $P_{wb}$  allows us to derive the above-employed empirical formula of  $\phi_b = 1.33 + 4.39(T_e - 0.33)$  with the Taylor expansion in the above-described parameter regime of the high-potential mode [Fig. 1(a)], for instance.

## 5. Scaling Law of Potential Formation with ECH Powers

Summarized data on  $\phi_c$  [kV] (or  $\phi_b$  due to Fig. 1) as a function of *externally controllable* plug ECH powers,  $P_{ECH}$  [kW], and  $n_c$  [ $10^{18} \text{ m}^{-3}$ ] are plotted in Fig. 3 along with the solid curves from *the empirical scaling* of  $\phi_c = 1.73 \times 10^{-4} P_{ECH}^{1.73} \exp(-0.33n_c)$ . According to the scaling, further favorable increase in confining potentials is anticipated with installing more powerful ECH sources beyond the power limit in Fig. 3. Experiments beyond 200-kW ECH injection into tandem-mirror plasmas have never been tried all through the tandem-mirror history.

*An assumption of the validity of extrapolation of the experimentally verified scaling theories and relations* allows us to make a scenario in search of innovative tandem fusion researches.

The combination of physically well interpreted scalings of (i) the strong ECH relation extended over both high-potential and hot-ion modes with the key parameters of  $\phi_c$ ,  $\phi_b$ ,  $T_e$ , and  $n_p/n_c$  [5] [*i.e.*,  $\phi_c=c_1 f_1(T_e, \phi_b, n_p/n_c)$  using the functional dependence of  $f$  with a constant  $c$  (Sections 3 and 4)], (ii) the scaling of the effect of  $\phi_b$  on  $T_e$  [*i.e.*,  $T_e=c_2 f_2(\phi_b)$ ], having the consistency with the electron energy-balance equation (Section 4), (iii) the empirical ECH power scaling for the formation of  $\phi_c$  (or  $\phi_b$  with  $n_p/n_c$  via Fig. 1) [*i.e.*,  $\phi_c$  or  $\phi_b=c_3 f_3(P_{ECH}, n_c$  or  $n_p/n_c)$ ], on the basis of an electron feeding effect due to  $P_{ECH}$  from plug to barrier regions (Section 5)], and (iv) the Pastukhov relation with  $\phi_c$ ,  $\phi_b$ ,  $T_i$ ,  $T_e$  and  $n_c$  [6]. A substitution of the scaling (ii) of  $T_e$  into  $f_1$  in (i), and then the use of the scaling (iii) of  $\phi_b$  in (i) provides the scaling of  $\phi_c$  with  $P_{ECH}$  in Fig. 4 [*i.e.*,  $\phi_c=c_4 f_4(P_{ECH}, n_p/n_c)$ ]. (v) Consequently, under the assumption of the validity of the extension of the above-summarized scaling bases having the theoretical interpretations, the formation of Pastukhov's predicted  $\phi_c$  of 30 kV for confining  $Q=1$  plasmas (see Refs. [1 and 6]) is scaled to require 5-MW  $P_{ECH}$  with  $n_p/n_c=0.3$ ,  $T_i=16$  keV, and  $n_c\tau_E=2.5\times 10^{19}$  m<sup>-3</sup>s with a direct-converter efficiency of 0.8, for instance. For challenging these future possibilities, step-to-step works for verifying the validity of an order-of-magnitude extension should be made on the basis of these theoretically supported scalings and established knowledge in the individually realized parameter regime for the high-potential and hot-ion modes.

## 6. Summary

The scalings in the main tandem-mirror operations from 1979 to 2000 on GAMMA 10, characterized in terms of the high-potential mode having kV-order plasma-confining potentials, and the hot-ion mode yielding fusion neutrons from bulk ions with  $T_i=10$ -20 keV, are consolidated and generalized. In particular, the novel proposal of the combination of Cohen's strong ECH and Pastukhov's potential-confinement theories provides the generalized physics interpretations covering over both modes upon the observed scalings; that is, the scalings of potential formation and the associated potential effects on improvements in plasma parameters (*i.e.*,  $T_e$ ,  $T_i$  [1],  $n_c$ ,  $\tau_E$  due to the formation of  $\phi_b$  and  $\phi_c$  with  $P_{ECH}$ ) for exploring the future upgraded modes under the extension of these theoretically supported scaling bases.

## References

- [1] MIYOSHI, S., et al., in Plasma Physics and Controlled Nuclear Fusion Research (Proc. 13th Int. Conf. Washington D.C., 1990) Vol. 2, IAEA, Vienna (1991) 539.
- [2] CHO, T., et al., Phys. Rev. Lett. **64** (1990) 1373; Phys. Rev. A **45** (1992) 2532.
- [3] KIWAMOTO, Y., et al., Phys. Plasmas **3** (1996) 578.
- [4] YATSU, K., et al., Nucl. Fusion **39** (1999) 1707.
- [5] COHEN, R. H., Phys. Fluids **26** (1983) 2774.
- [6] PASTUKHOV, V. P., Nucl. Fusion **14** (1974) 3.

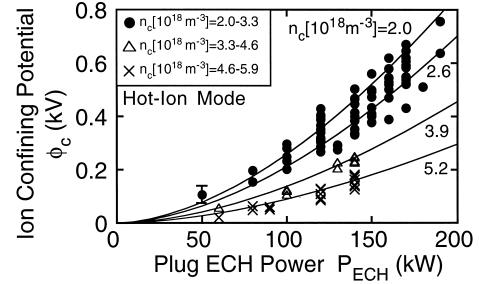


FIG. 3. The scaling of  $\phi_c$  with  $P_{ECH}$  as a function of  $n_c$  (the hot-ion mode).

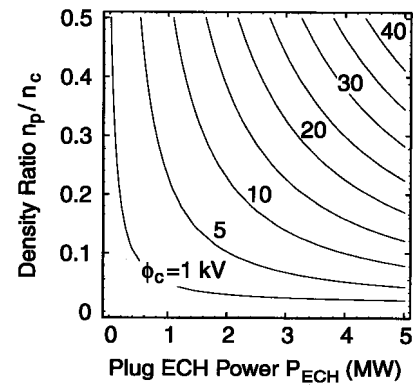


FIG. 4. The scaling of  $\phi_c$  in relation to  $P_{ECH}$  and  $n_p/n_c$ .